

Role of magnetic ions in the thermal Hall effect of the paramagnetic insulator TmVO₄

Ashvini Vallipuram^{*,1,†} Lu Chen^{*,1,‡} Emma Campillo,¹ Manel Mezidi,^{1,2} Gaël Grissonnanche,^{3,4}

Mark P. Zic,⁵ Yuntian Li,⁶ Ian R. Fisher,⁶ Jordan Baglo,¹ and Louis Taillefer^{1,7,§}

¹*Institut quantique, Département de physique & RQMP,*

Université de Sherbrooke, Sherbrooke, Québec J1K 2R1 Canada

²*Université Paris-Cité, Laboratoire Matériaux et Phénomènes Quantiques, CNRS (UMR 7162), 75013 Paris, France*

³*Laboratory of Atomic and Solid State Physics, Cornell University, Ithaca, NY 14853, USA*

⁴*Kavli Institute at Cornell for Nanoscale Science, Ithaca, NY 14853, USA*

⁵*Geballe Laboratory for Advanced Materials and Department of Physics, Stanford University, CA 94305, USA*

⁶*Geballe Laboratory for Advanced Materials and Department of Applied Physics, Stanford University, CA 94305, USA*

⁷*Canadian Institute for Advanced Research, Toronto, Ontario M5G 1M1, Canada*

(Dated: March 5, 2024)

In a growing number of materials, phonons have been found to generate a thermal Hall effect, but the underlying mechanism remains unclear. Inspired by previous studies that revealed the importance of Tb³⁺ ions in generating the thermal Hall effect in a family of pyrochlores, we investigated the role of Tm³⁺ ions in TmVO₄, a paramagnetic insulator with a different crystal structure. We observe a negative thermal Hall conductivity in TmVO₄ with a magnitude such that the Hall angle, $|\kappa_{xy}/\kappa_{xx}|$, is approximately 1×10^{-3} at $H = 15$ T and $T = 20$ K, typical for a phonon-generated thermal Hall effect. In contrast to the negligible κ_{xy} found in the nonmagnetic pyrochlore analog (where the Tb³⁺ ions are replaced with Y³⁺), we observe a negative κ_{xy} in YVO₄ with a Hall angle of magnitude comparable to that of TmVO₄. This shows that the Tm³⁺ ions are not essential for the thermal Hall effect in this family of materials. Interestingly, at an intermediate Y concentration of $x = 0.3$ in Tm_{1-x}Y_xVO₄, κ_{xy} was found to have a positive sign, pointing to the importance of impurities in the thermal Hall effect of phonons.

I. INTRODUCTION

In the last decade, a thermal Hall effect has been measured in a number of insulators where phonons are the main heat carriers, including multiferroics such as Fe₂Mo₃O₈ [1], cuprates such as La₂CuO₄ [2, 3] and Nd₂CuO₄ [4], nonmagnetic SrTiO₃ [5] and the antiferromagnet Cu₃TeO₆ [6], see Fig. 1. In Tb₃Ga₅O₁₂ [7], the first insulator in which a thermal Hall signal was detected, the effect was attributed to skew scattering of phonons by superstoichiometric Tb⁺³ impurities [8].

Since then, a number of theoretical scenarios have been proposed to explain the origin of the phonon thermal Hall effect. Some attribute the thermal Hall conductivity κ_{xy} to the Berry curvature of phonon bands [9]. Others link it to various types of spin-lattice coupling [10–13]. In yet others, the role of impurities is considered important [14–16]. But it remains unclear which of these scenarios applies to what material.

In a previous study on pyrochlores [17], a sizeable κ_{xy} was observed in Tb₂Ti₂O₇ but a negligible κ_{xy} was detected in Y₂Ti₂O₇. Although the κ_{xy} signal in Tb₂Ti₂O₇ was originally attributed to some exotic neutral excitations linked to the spin-liquid nature of the system [17], it was later argued that phonons are in fact responsible for the thermal Hall effect in this ma-

terial [18], since a κ_{xy} signal of comparable magnitude is still observed when 70% of the Tb³⁺ ions are replaced by Y³⁺ ions, and the spin state of the system is profoundly altered. Irrespective of the underlying mechanism, this study does show that Tb³⁺ ions are essential for generating a thermal Hall effect in these pyrochlores.

Here we report a similar study carried out on a different oxide, TmVO₄, wherein we investigate what happens to the thermal Hall effect when we substitute the magnetic ion Tm³⁺ for the nonmagnetic ion Y³⁺.

The insulator TmVO₄ exhibits a rich set of phenomena at low temperatures. It undergoes a cooperative Jahn-Teller phase transition at $T = T_D \simeq 2$ K in zero field, and at $H = H_D \simeq 0.5$ T at $T = 0$ (for $H//c$) [23]. (Note that we use H as a shorthand notation for $\mu_0 H$.) The ordered state consists of a simultaneous ferroquadrupole order of the local 4f electronic orbitals of each Tm atom, accompanied by a structural transition, by which the crystal structure goes from tetragonal at high temperatures (I41/amd spacegroup [21]) to orthorhombic at low temperatures [23–27]. However, no magnetically ordered state has been reported in TmVO₄ [23]. Our own study will focus on temperatures above T_D .

II. METHODS

A. Samples

The following three rare-earth vanadates were studied: TmVO₄, YVO₄ and Tm_{0.7}Y_{0.3}VO₄. The samples were grown using a flux growth method [28, 29]. They are nee-

[†] * A.V. and L.C. contributed equally to this work.;
ashvini.vallipuram@usherbrooke.ca

[‡] lu.chen@usherbrooke.ca

[§] louis.taillefer@usherbrooke.ca

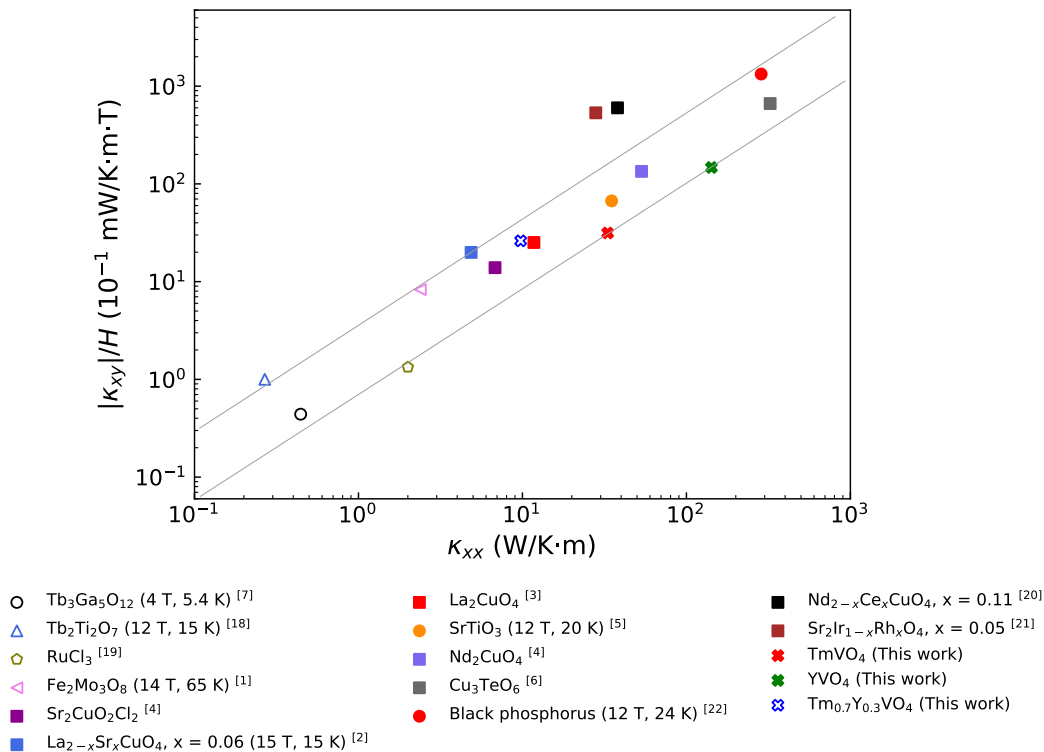


FIG. 1. Phonon thermal Hall conductivity normalized by field, $|\kappa_{xy}|/H$ of various insulators [1, 3–7, 18–21] as a function of their thermal conductivity, κ_{xx} . The data are taken at $H = 15$ T and $T = 20$ K unless indicated otherwise. This figure is inspired from a similar plot from Li et al. [22] with the values of our three samples added. The grey lines mark the region where most values of κ_{xy} are found, showing that κ_{xy} scales with κ_{xx} , as emphasized previously [1, 2, 6, 22]. The two data points that lie above the delimited region are $\text{Nd}_{2-x}\text{Ce}_x\text{CuO}_4$: $x = 0.11$ [20] and $\text{Sr}_2\text{Ir}_{1-x}\text{Rh}_x\text{O}_4$: $x = 0.05$ [21] (see text). Open (full) symbols indicate a positive (negative) κ_{xy} .

dle shaped with their long axis along the c axis, which is the easy axis of magnetization [30]. Because TmVO_4 has a large anisotropy in its g -factor ($g_c = 10$ & $g_a = g_b = 0$) [31], even a slight misalignment of the magnetic field can cause a large torque on the sample, which can detach from its mount.

Two measures were adopted to prevent this. First, the thermal transport contacts on TmVO_4 and $\text{Tm}_{0.7}\text{Y}_{0.3}\text{VO}_4$ samples were made with silver epoxy to ensure strong contacts that would adhere to a very smooth surface and wouldn't peel off. These contacts were solidified for about 10 minutes on a hot plate at 150 °C. Note that the contacts on the YVO_4 samples were done with silver paint, since there is no magnetic torque in this case. For the heater contact, a 50 μm diameter silver wire was used and for the thermal transport contacts, wires with a diameter of 25 μm were used.

In addition, a small wood stick was positioned along the TmVO_4 and $\text{Tm}_{0.7}\text{Y}_{0.3}\text{VO}_4$ samples, and was linked to the sample by the heater wire. The thermal conductivity κ_{xx} was measured with and without the wood stick and only a 5 % (8 %) difference was observed at the peak temperature for TmVO_4 ($\text{Tm}_{0.7}\text{Y}_{0.3}\text{VO}_4$). The sample dimensions (contact dimensions) are given in Table I.

B. Thermal transport measurements

To perform a conventional thermal transport study, a 5-contact measurement is done using a steady-state method at a fixed field, as sketched in Fig. 2. A heat current (\vec{J}) is generated along the x axis from the heater contact on one end of the sample and the copper block on the other end. The heater is a strain gauge of 5 k Ω whose resistance does not change with temperature or field. (No potential strain is conferred to the sample since the heater is glued with GE varnish to a silver pad.) This heat current was applied along the c axis of the sample (the x axis in Fig. 2), while the field H was applied along the a axis (the z axis in Fig. 2). Note that the field ($H = 10$ or 15 T) was applied at high temperatures (at 83 K) and the samples were cooled down to $\simeq 3$ K using a variable temperature insert (VTI). This procedure ensures that no hysteresis due to the sample is generated.

Temperature steps from $\simeq 3$ K to 80 K were done at fixed fields and all the temperature signals were stable before measuring each temperature difference (ΔT_x and ΔT_y in Fig. 2) using type-E (chromium/constantan) thermocouples. Note that a test has been done previously to show that thermocouples and chip-based ther-

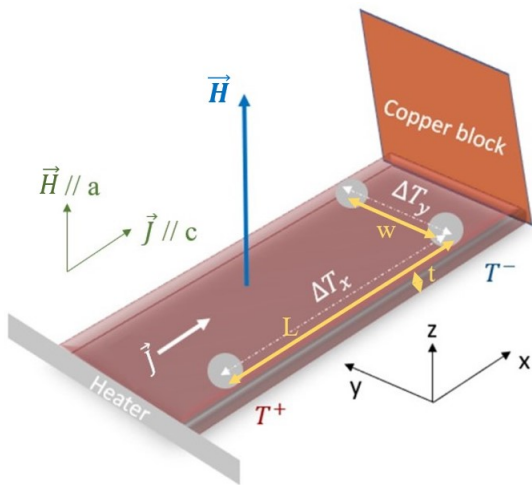


FIG. 2. Experimental setup used to measure κ_{xx} and κ_{xy} . A heat current J is generated along the x axis (c axis of the sample) and a magnetic field H is applied perpendicular to it, along the z axis (a axis of the sample). Differences in temperature are measured along the x axis (longitudinal temperature difference, $\Delta T_x = T^+ - T^-$) and the y axis (transverse temperature difference, ΔT_y).

mometers (Cernox) yield the same thermal Hall data (see Appendix C in ref. [32]). Also, note that for all the voltages, the background voltage (when the heat is off) is subtracted from the measured signal (when the heat is on).

The conductivities κ_{xx} and κ_{xy} were measured as described elsewhere [2–4]. Note that the transverse temperature difference ΔT_y is obtained by measuring in both field polarities ($+H$ and $-H$). We have checked that our technique is independent of the particular choice of sequence, i.e., whether we measure $+H$ first and then $-H$ or if we measure instead $-H$ first and then $+H$. This means that our experimental setup and our procedure do not generate any (technique dependent) hysteresis. Then, we antisymmetrize the measured signals to get rid of any longitudinal contribution due to a possible slight misalignment of the transverse contacts:

$$\Delta T_y(H) = [\Delta T_y(T, H) - \Delta T_y(T, -H)]/2 \quad (1)$$

The sign of ΔT_y is determined by measuring a sample of known κ_{xy} with the same setup and wiring. In a metallic sample with Hall coefficient $R_H > 0$ (thus an electrical Hall conductivity $\sigma_{xy} > 0$), the thermal Hall

	L (mm)	w (mm)	t (mm)
TmVO ₄	0.66	0.24	0.04
YVO ₄	0.49	0.25	0.06
Tm _{0.7} Y _{0.3} VO ₄	0.65	0.45	0.04

TABLE I. Dimensions of the three samples investigated here. L = length between contacts; w = width of the sample; t = thickness of the sample.

conductivity κ_{xy} will be positive (at least in the $T = 0$ limit) since both thermal and electrical conductivities are related by the Wiedemann–Franz law : $\kappa_{xy}/T = L_0\sigma_{xy}$ for $T \rightarrow 0$.

The thermal conductivity is defined as:

$$\kappa_{xx} = \frac{\dot{Q}}{\Delta T_x \cdot \alpha} \quad (2)$$

where \dot{Q} is the heating power and α is a geometric factor ($\alpha = \frac{w \cdot t}{L}$; see Table I for sample dimensions). The thermal Hall conductivity is defined as:

$$\kappa_{xy} = \kappa_{yy} \left(\frac{\Delta T_y}{\Delta T_x} \right) \left(\frac{L}{w} \right) \quad (3)$$

Note that here we assume that $\kappa_{yy} = \kappa_{xx}$ (i.e. that $\kappa_a = \kappa_c$), but this is not quite right since the c -axis conductivity is not identical to the a -axis conductivity. This implies that the amplitude of κ_{xy} reported here is not quite accurate, and would need to be multiplied by the anisotropy factor κ_a/κ_c . Given the needle shape of our samples, measurements with $J//a$ have not been done.

III. RESULTS

A. Thermal conductivity, κ_{xx}

The thermal conductivity κ_{xx} of our three samples is displayed in Fig. 3. All three curves are typical of insulators, with a peak near $T \simeq 20 - 30$ K.

The thermal conductivity of TmVO₄ was measured previously [33]. These early measurements were done with $J//H//c$ (along the easy axis [30]) for $H < 7$ T and for $T < 30$ K, whereas our measurements were done with $J//c$ and $H//a$, covering a larger temperature and field range. This previous study reports a slightly higher κ_{xx} peak, perhaps due to larger samples and higher sample quality. The field increased κ_{xx} at low temperatures ($T < 6$ K).

In our study, we also see an increase in κ_{xx} with H at low temperatures ($T < 10$ K; inset of Fig. 4a).

The zero-field curves are compared in Fig. 3(d), where we see that κ_{xx} in YVO₄ is much larger than in the other two samples. The magnitude of κ_{xx} in the stoichiometric sample of paramagnetic TmVO₄ is much lower presumably because phonons scatter on the crystal field levels of the Tm³⁺ ions. This is also presumed to be the case in the frustrated spin system Tb₂Ti₂O₇, where the scattering of phonons would involve the crystal field levels of the Tb³⁺ ions, as argued previously [8]. This scattering process is much stronger for Tb³⁺ than Tm³⁺, resulting in a value of $\kappa_{xx} \simeq 2$ W/m·K at $T = 20$ K in Tb₂Ti₂O₇ [34], compared to $\kappa_{xx} \simeq 40$ W/m·K in TmVO₄ (Fig. 3(a)).

As in the case of Tb₂Ti₂O₇, where the field dependence of κ_{xx} is exceptionally strong [34], we view the

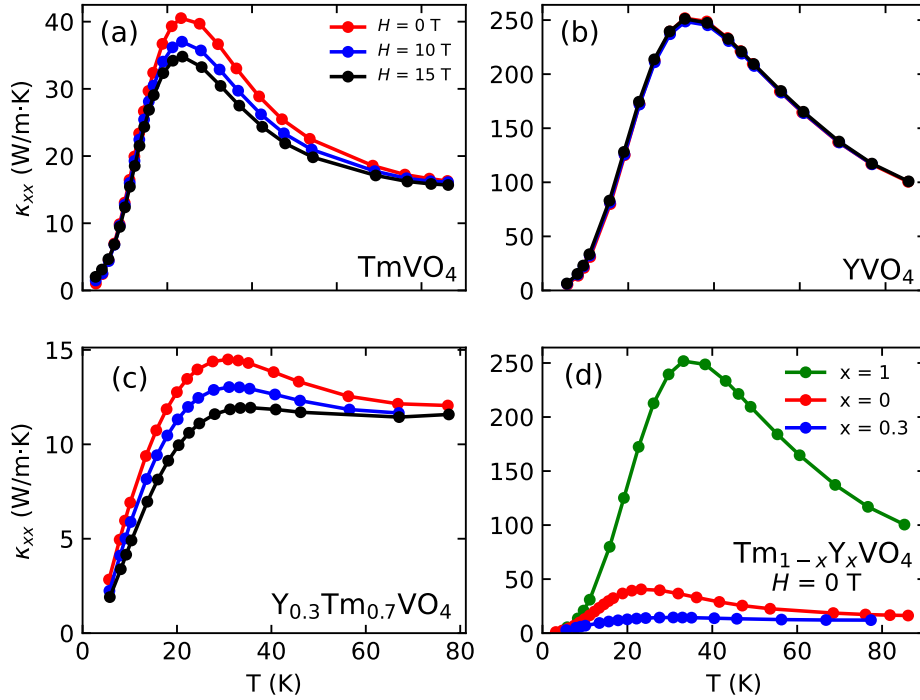


FIG. 3. Thermal conductivity of TmVO_4 (a), YVO_4 (b) and $\text{Tm}_{0.7}\text{Y}_{0.3}\text{VO}_4$ (c) as a function of temperature, measured with a heat current $J//c$ and a magnetic field $H//a$ ($H \perp J$, for $H = 0$ (red), 10 T (blue) and 15 T (black)). (d) Comparison of the three conductivities at $H = 0$. We see that substituting Y for Tm causes a major reduction in κ_{xx} , which is then further reduced if Y impurities are added.

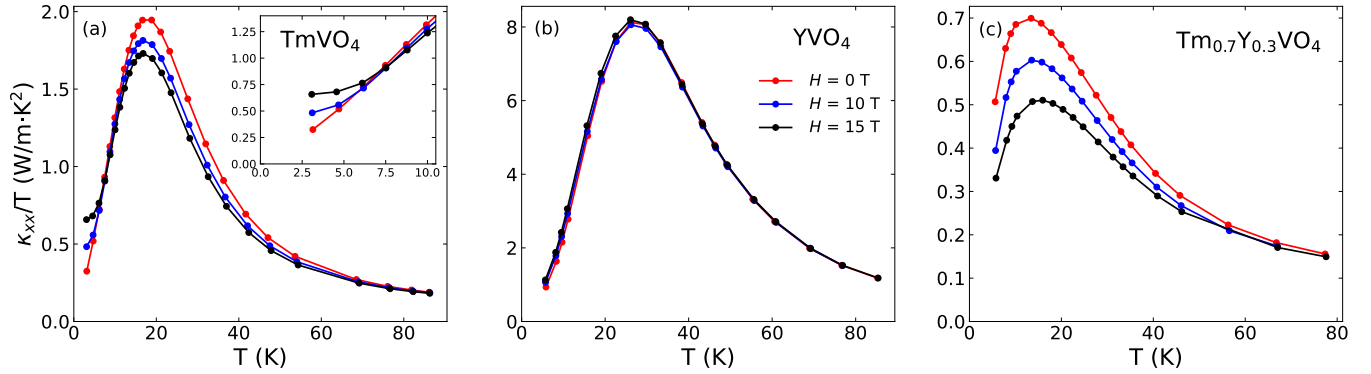


FIG. 4. Thermal conductivity of TmVO_4 (a), YVO_4 (b) and $\text{Tm}_{0.7}\text{Y}_{0.3}\text{VO}_4$ (c), for different applied magnetic fields, as indicated, plotted as κ_{xx}/T vs T to emphasize the low temperature regime. Note the strong field dependence in the two samples that contain Tm^{3+} ions, compared to the much weaker field dependence in YVO_4 . In panel (a), the inset shows a zoom below 10 K, where we see a different regime of H dependence, with a strong increase in κ_{xx} with increasing H .

sizable field dependence of κ_{xx} in TmVO_4 (Fig. 3(a)) and $\text{Tm}_{0.7}\text{Y}_{0.3}\text{VO}_4$ (Fig. 3(c)), as a confirmation that phonons are scattered by the crystal field levels of the Tm^{3+} ions. The weaker field dependence seen in YVO_4 (Fig. 3(b)) is consistent with that picture. We attribute the fact that κ_{xx} in $\text{Tm}_{0.7}\text{Y}_{0.3}\text{VO}_4$ is even smaller than in TmVO_4 to the extra disorder introduced by the Y impurities (Fig. 3(d)).

In Fig. 4, we plot κ_{xx}/T vs T , to emphasize the data

at low temperature. We see that below ~ 10 K or so, the field dependence of κ_{xx} in TmVO_4 becomes very strong and opposite in sign relative to its behaviour at higher temperature (inset of Fig. 4(a)). We speculate that this change of behaviour is associated with the quadratic splitting of the crystal field levels of the Tm^{3+} ions with field (second order Zeeman interaction for $H//a$) [23] which changes the resonant phonon scattering (for phonons of appropriate symmetry).

Interestingly, this change in field dependence as the temperature is raised was actually captured by theoretical calculations that consider the main scattering mechanism of phonons to be resonant scattering on electronic levels of the Tm^{3+} ions [35, 36], albeit for temperatures much closer to the transition.

B. Thermal Hall conductivity, κ_{xy}

The thermal Hall conductivity κ_{xy} of our three samples is displayed in Fig. 5. Only data at $H = 15$ T are shown, but data at $H = 10$ T were also taken; they are similar but smaller in magnitude, roughly in proportion to the field amplitude. The first observation is that all three samples exhibit a non-negligible thermal Hall conductivity. The surprise is that the sign of κ_{xy} is negative in the two stoichiometric materials, TmVO_4 and YVO_4 , but it is positive in the disordered sample $\text{Tm}_{0.7}\text{Y}_{0.3}\text{VO}_4$.

We see that the temperature at which $\kappa_{xy}(T)$ peaks (Fig. 5) is the same as the temperature at which the phonon-dominated $\kappa_{xx}(T)$ peaks (Fig. 3), for example $\simeq 25$ K in TmVO_4 and $\simeq 35$ K in YVO_4 . As argued before for other materials [4–6, 22], this is an argument in support of phonons being the heat carriers responsible for the thermal Hall signal in these materials.

Looking at Fig. 5, we also notice that the magnitude of κ_{xy} appears to roughly scale with the magnitude of κ_{xx} seen in Fig. 3d. This is confirmed when looking at the thermal Hall angle, plotted as $|\kappa_{xy}/\kappa_{xx}|$ vs T in Fig. 6. Indeed, we see that $|\kappa_{xy}/\kappa_{xx}| \simeq 1 \times 10^{-3}$ at $T \sim 20$ K in both YVO_4 and $\text{Tm}_{0.7}\text{Y}_{0.3}\text{VO}_4$, even though the magnitude of κ_{xy} is 25 times larger in YVO_4 (Fig. 5). This is because κ_{xx} is also roughly 25 times larger in

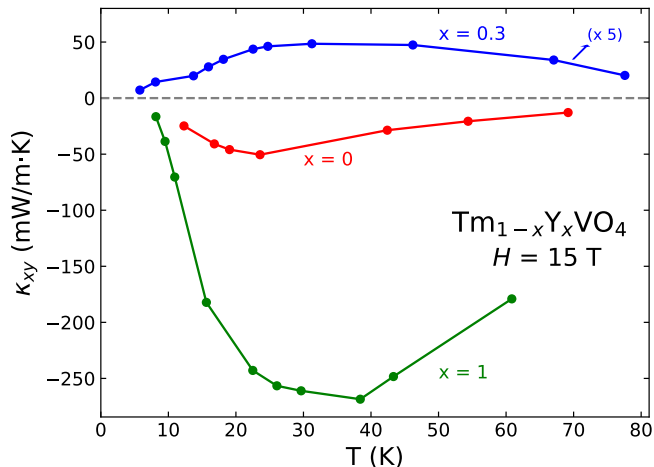


FIG. 5. Thermal Hall conductivity of TmVO_4 (red), YVO_4 (green) and $\text{Tm}_{0.7}\text{Y}_{0.3}\text{VO}_4$ (blue) as a function of temperature, measured with a heat current $J//c$ and a magnetic field $H//a$ ($H \perp J$), at $H = 15$ T. Note that κ_{xy} for $\text{Tm}_{0.7}\text{Y}_{0.3}\text{VO}_4$ has been multiplied by a factor of 5.

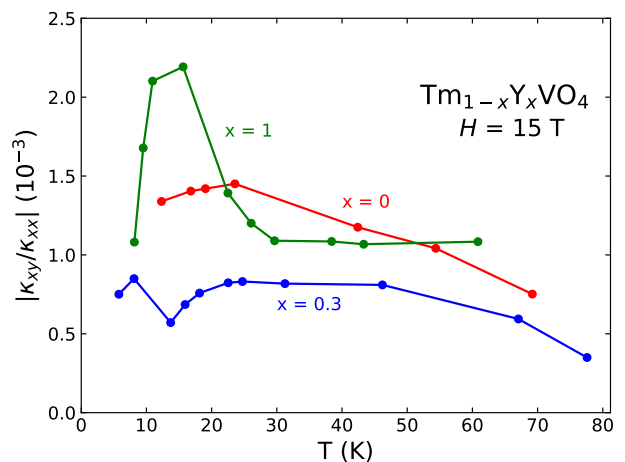


FIG. 6. Thermal Hall angle of TmVO_4 (red), YVO_4 (green) and $\text{Tm}_{0.7}\text{Y}_{0.3}\text{VO}_4$ (blue), plotted as $|\kappa_{xy}/\kappa_{xx}|$ vs T , for $H = 15$ T. At $T = 20$ K, the obtained value is around 1×10^{-3} for all three materials, a magnitude typical of the phonon Hall effect in several insulators [6, 22].

YVO_4 (Fig. 3).

IV. DISCUSSION

In the pyrochlore study, a non-zero (and positive) thermal Hall effect was measured in $\text{Tb}_2\text{Ti}_2\text{O}_7$, but a negligible κ_{xy} was detected in $\text{Y}_2\text{Ti}_2\text{O}_7$ [17]. It was initially speculated that the thermal Hall signal in $\text{Tb}_2\text{Ti}_2\text{O}_7$ was due to some exotic spin excitations [17]. However, a subsequent study found that the κ_{xy} signal remains as strong when 70% of the magnetic Tb^{3+} ions are replaced by nonmagnetic Y^{3+} ions, thereby dramatically altering the frustrated spin-liquid state of pure $\text{Tb}_2\text{Ti}_2\text{O}_7$ [18]. This led to the conclusion that phonons are in fact the heat carriers responsible for the thermal Hall effect in these pyrochlores. Moreover, the fact that κ_{xy} becomes negligible in $\text{Y}_2\text{Ti}_2\text{O}_7$, when all Tb is replaced by Y, indicates that magnetism plays a key role in the generation of the phonon thermal Hall effect in these pyrochlores.

Turning to our own study, we also observe a non-zero κ_{xy} in TmVO_4 , another oxide with magnetic ions (Tm^{3+}), and we also attribute this Hall effect to phonons, as argued above. In our comparison with $\text{Tb}_2\text{Ti}_2\text{O}_7$, we see two differences. The first is the fact that our nonmagnetic parent compound, YVO_4 , also displays a non-zero κ_{xy} , unlike the negligible signal of $\text{Y}_2\text{Ti}_2\text{O}_7$. So in these vanadates, the phonon Hall effect does not depend crucially on the magnetic moment associated with Tm^{3+} ions. Note that a non-zero thermal Hall effect from phonons has been observed in other nonmagnetic insulators, such as strontium titanate [5] and black phosphorous [22].

The second difference is the sign of κ_{xy} : positive in $\text{Tb}_2\text{Ti}_2\text{O}_7$, negative in TmVO_4 . The sign of the phonon

Hall conductivity is an entirely open question, on which existing theories shed little light. Phenomenologically, both signs are observed, see Fig. 1. For example, the phononic κ_{xy} is negative in SrTiO₃ [5], Cu₃TeO₆ [6] and black phosphorus [22], as well as in all cuprates, whether undoped [3, 4], hole-doped [2] or electron-doped [20]. A positive phononic κ_{xy} is observed in Fe₂Mo₃O₈ [1], (Tb_{0.3}Y_{0.7})₂Ti₂O₇ [18] and RuCl₃ [19, 37]. A remarkable feature of our findings is that κ_{xy} changes sign to positive upon introducing 30% Y into TmVO₄ (Fig. 5). This suggests that impurities, in much larger concentration in Tm_{0.7}Y_{0.3}VO₄ relative to either TmVO₄ or YVO₄, is an important ingredient for the generation of a phonon thermal Hall effect.

It is instructive to look at the magnitude of κ_{xy} . As argued by others [1, 6, 22], the relevant quantity for this is the ratio κ_{xy}/κ_{xx} , namely the Hall angle. In Fig. 6, we see that in our three samples $|\kappa_{xy}/\kappa_{xx}| \simeq 1 \times 10^{-3}$ at $T = 20$ K and $H = 15$ T. This is quite typical. Indeed, the cuprate Mott insulators La₂CuO₄, Nd₂CuO₄ and Sr₂CuO₂Cl₂ and the antiferromagnetic insulator Cu₃TeO₆ all have a Hall angle of about 3×10^{-3} at the same temperature and field [6]. The Kitaev spin liquid candidate RuCl₃ has a Hall angle of about 1×10^{-3} . Note that the magnitude of κ_{xy} varies by three orders of magnitude across those various materials.

It is worth noting that significantly larger thermal Hall angles have been observed in two cases so far: the Ce-doped cuprate Nd₂CuO₄ [20] and the Rh-doped iridate Sr₂IrO₄ [21]. In as-grown samples of Nd₂CuO₄ with 11% Ce and Sr₂IrO₄ with 5% Rh, $|\kappa_{xy}/\kappa_{xx}| \simeq 30 \times 10^{-3}$ at $T = 20$ K and $H = 15$ T. Both materials are insulators with antiferromagnetic order at these dopings, and it was argued in the latter study that impurities embedded in an antiferromagnetic environment strongly promote the phonon thermal Hall effect [21], as suggested theoretically for a mechanism of resonant side-jump scattering

of phonons [16].

V. SUMMARY

We have measured a non-zero thermal Hall conductivity κ_{xy} in the vanadates TmVO₄, YVO₄ and Tm_{0.7}Y_{0.3}VO₄. All evidence points to phonons as the heat carriers responsible for generating this Hall effect. The magnitude of the Hall response is similar in all three, with a Hall angle of $|\kappa_{xy}/\kappa_{xx}| \simeq 1 \times 10^{-3}$ at $T = 20$ K and $H = 15$ T, comparable to the phonon Hall effect in several insulating materials. This shows that Tm³⁺ ions do not play an essential role in generating the Hall effect in these rare-earth vanadates. While the sign of κ_{xy} in the two stoichiometric compounds TmVO₄ and YVO₄ is negative, we find a positive sign in the more disordered Tm_{0.7}Y_{0.3}VO₄. This points to a special role played by impurities in this family of materials.

ACKNOWLEDGMENTS

We thank S. Fortier for his assistance with the experiments. L. T. acknowledges support from the Canadian Institute for Advanced Research (CIFAR) as a CIFAR Fellow and funding from the Institut Quantique, the Natural Sciences and Engineering Research Council of Canada (NSERC; PIN:123817), the Fonds de Recherche du Québec - Nature et Technologies (FRQNT), the Canada Foundation for Innovation (CFI), and a Canada Research Chair. This research was undertaken thanks in part to funding from the Canada First Research Excellence Fund.

Crystal growth and characterization performed at Stanford University was supported by the Air Force Office of Scientific Research under award number FA9550-20-1-0252. MPZ was also partially supported by a National Science Foundation Graduate Research Fellowship under grant number DGE-1656518.

-
- [1] T. Ideue, T. Kurumaji, S. Ishiwata, and Y. Tokura, Giant thermal Hall effect in multiferroics, *Nature Materials* **16**, 797 (2017).
- [2] G. Grissonnanche, A. Legros, S. Badoux, E. Lefrançois, V. Zlatko, M. Lizaire, F. Laliberté, A. Gourgout, J.-S. Zhou, S. Pyon, T. Takayama, H. Takagi, S. Ono, N. Doiron-Leyraud, and L. Taillefer, Giant thermal Hall conductivity in the pseudogap phase of cuprate superconductors, *Nature* **571**, 376 (2019).
- [3] G. Grissonnanche, S. Thériault, A. Gourgout, M.-E. Boulanger, E. Lefrançois, A. Ateaï, F. Laliberté, M. Dion, J.-S. Zhou, S. Pyon, T. Takayama, H. Takagi, S. Ono, N. Doiron-Leyraud, and L. Taillefer, Chiral phonons in the pseudogap phase of cuprates, *Nature Physics* **16**, 1108 (2020).
- [4] M.-E. Boulanger, G. Grissonnanche, S. Badoux, A. Alaire, E. Lefrançois, A. Legros, A. Gourgout, M. Dion, C. H. Wang, X. H. Chen, R. Liang, W. N. Hardy, D. A. Bonn, and L. Taillefer, Thermal Hall conductivity in the cuprate Mott insulators Nd₂CuO₄ and Sr₂CuO₂Cl₂, *Nature Communications* **11**, 5325 (2020).
- [5] X. Li, B. Fauqué, Z. Zhu, and K. Behnia, Phonon thermal Hall effect in strontium titanate, *Physical Review Letters* **124**, 105901 (2020).
- [6] L. Chen, M.-E. Boulanger, Z.-C. Wang, F. Tafti, and L. Taillefer, Large phonon thermal Hall conductivity in the antiferromagnetic insulator Cu₃TeO₆, *Proceedings of the National Academy of Sciences* **119**, e2208016119 (2022).
- [7] C. Strohm, G. L. J. A. Rikken, and P. Wyder, Phenomenological evidence for the phonon Hall effect, *Physical Review Letters* **95**, 155901 (2005).
- [8] M. Mori, A. Spencer-Smith, O. P. Sushkov, and S. Maekawa, Origin of the phonon Hall effect in rare-earth garnets, *Physical Review Letters* **113**, 265901 (2014).
- [9] T. Qin, J. Zhou, and J. Shi, Berry curvature and the

- phonon Hall effect, *Physical Review B* **86**, 104305 (2012).
- [10] M. Ye, L. Savary, and L. Balents, Phonon Hall viscosity in magnetic insulators, arXiv [Preprint] (2021), arXiv:2103.04223.
- [11] Y. Zhang, Y. Teng, R. Samajdar, S. Sachdev, and M. S. Scheurer, Phonon Hall viscosity from phonon-spinon interactions, *Physical Review B* **104**, 035103 (2021).
- [12] R. Samajdar, S. Chatterjee, S. Sachdev, and M. S. Scheurer, Thermal Hall effect in square-lattice spin liquids: A Schwinger boson mean-field study, *Physical Review B* **99**, 165126 (2019).
- [13] L. Mangeolle, L. Balents, and L. Savary, Phonon thermal Hall conductivity from scattering with collective fluctuations, *Physical Review X* **12**, 041031 (2022).
- [14] H. Guo and S. Sachdev, Extrinsic phonon thermal Hall transport from Hall viscosity, *Physical Review B* **103**, 205115 (2021).
- [15] X.-Q. Sun, J.-Y. Chen, and S. A. Kivelson, Large extrinsic phonon thermal Hall effect from resonant scattering, *Physical Review B* **106**, 144111 (2022).
- [16] H. Guo, D. G. Joshi, and S. Sachdev, Resonant thermal Hall effect of phonons coupled to dynamical defects, *Proceedings of the National Academy of Sciences* **119**, e2215141119 (2022).
- [17] M. Hirschberger, J. W. Krizan, R. J. Cava, and N. P. Ong, Large thermal Hall conductivity of neutral spin excitations in a frustrated quantum magnet, *Science* **348**, 106 (2015).
- [18] Y. Hirokane, Y. Nii, Y. Tomioka, and Y. Onose, Phononic thermal Hall effect in diluted terbium oxides, *Physical Review B* **99**, 134419 (2019).
- [19] E. Lefrançois, G. Grissonnanche, J. Baglo, P. Lampen-Kelley, J.-Q. Yan, C. Balz, D. Mandrus, S. E. Nagler, S. Kim, Y.-J. Kim, N. Doiron-Leyraud, and L. Taillefer, Evidence of a phonon Hall effect in the Kitaev spin liquid candidate α - RuCl_3 , *Physical Review X* **12**, 021025 (2022).
- [20] M.-E. Boulanger, G. Grissonnanche, E. Lefrançois, A. Gourgout, K.-J. Xu, Z.-X. Shen, R. L. Greene, and L. Taillefer, Thermal Hall conductivity of electron-doped cuprates, *Physical Review B* **105**, 115101 (2022).
- [21] A. Ataei, G. Grissonnanche, M.-E. Boulanger, L. Chen, E. Lefrançois, V. Brouet, and L. Taillefer, Phonon chirality from impurity scattering in the antiferromagnetic phase of Sr_2IrO_4 , *Nature Physics* (2024).
- [22] X. Li, Y. Machida, A. Subedi, Z. Zhu, L. Li, and K. Behnia, The phonon thermal Hall angle in black phosphorus, *Nature Communications* **14**, 1027 (2023).
- [23] I. Vinograd, K. R. Shirer, P. Massat, Z. Wang, T. Kissikov, D. Garcia, M. D. Bachmann, M. Horvatić, I. R. Fisher, and N. J. Curro, Second order Zeeman interaction and ferroquadrupolar order in TmVO_4 , *NPJ Quantum Materials* **7**, 1 (2022).
- [24] Z. Wang, I. Vinograd, Z. Mei, P. Menegasso, D. Garcia, P. Massat, I. R. Fisher, and N. J. Curro, Anisotropic nematic fluctuations above the ferroquadrupolar transition in TmVO_4 , *Physical Review B* **104**, 205137 (2021).
- [25] P. Massat, J. Wen, J. M. Jiang, A. T. Hristov, Y. Liu, R. W. Smaha, R. S. Feigelson, Y. S. Lee, R. M. Fernandes, and I. R. Fisher, Field-tuned ferroquadrupolar quantum phase transition in the insulator TmVO_4 , *Proceedings of the National Academy of Sciences* **119**, e2119942119 (2022).
- [26] Y.-H. Nian, I. Vinograd, T. Green, C. Chaffey, P. Massat, R. R. P. Singh, M. P. Zic, I. R. Fisher, and N. J. Curro, Spin-echo and quantum versus classical critical fluctuations in TmVO_4 , arXiv [Preprint] (2023), arXiv:2306.13244.
- [27] M. P. Zic, M. S. Ikeda, P. Massat, P. M. Hollister, L. Ye, E. W. Rosenberg, J. A. W. Straquadine, B. J. Ramshaw, and I. R. Fisher, Giant elastocaloric effect at low temperatures in TmVO_4 and implications for cryogenic cooling, arXiv [Preprint] (2023), arXiv:2308.15577.
- [28] R. Feigelson, Flux growth of type RVO_4 rare-earth vanadate crystals, *Journal of the American Ceramic Society* **51**, 538 (1968).
- [29] S. H. Smith and B. M. Wanklyn, Flux growth of rare earth vanadates and phosphates, *Journal of Crystal Growth* **21**, 23 (1974).
- [30] H. Suzuki, T. Inoue, and T. Ohtsuka, Enhanced nuclear cooling and spin-lattice relaxation time in TmVO_4 and TmPO_4 , *Physica B+C* **107**, 563 (1981).
- [31] A. H. Cooke, S. J. Swithenby, and M. R. Wells, The properties of thulium vanadate — An example of molecular field behaviour, *Solid State Communications* **10**, 265 (1972).
- [32] G. Grissonnanche, F. Laliberté, S. Dufour-Beauséjour, M. Matusiak, S. Badoux, F. F. Tafti, B. Michon, A. Ripopel, O. Cyr-Choinière, J. C. Baglo, B. J. Ramshaw, R. Liang, D. A. Bonn, W. N. Hardy, S. Krämer, D. LeBoeuf, D. Graf, N. Doiron-Leyraud, and L. Taillefer, Wiedemann-Franz law in the underdoped cuprate superconductor $\text{YBa}_2\text{Cu}_3\text{O}_y$, *Physical Review B* **93**, 064513 (2016).
- [33] B. Daudin and B. Salce, Thermal conductivity of rare earth vanadates and arsenates undergoing a cooperative Jahn-Teller effect, *Journal of Physics C: Solid State Physics* **15**, 463–475 (1982).
- [34] Q. J. Li, Z. Y. Zhao, C. Fan, F. B. Zhang, H. D. Zhou, X. Zhao, and X. F. Sun, Phonon-glass-like behavior of magnetic origin in single-crystal $\text{Tb}_2\text{Ti}_2\text{O}_7$, *Physical Review B* **87**, 214408 (2013).
- [35] W. Mutscheller and M. Wagner, Thermal conductivity of cooperative Jahn-Teller E-systems, *Physica Status Solidi (b)* **134**, 39 (1986).
- [36] W. Mutscheller and M. Wagner, The influence of magnetic fields on the thermal conductivity of the cooperative vibronic system TmVO_4 , *Physica Status Solidi (b)* **144**, 507 (1987).
- [37] R. Hentrich, M. Roslova, A. Isaeva, T. Doert, W. Brenig, B. Büchner, and C. Hess, Large thermal Hall effect in α - RuCl_3 : Evidence for heat transport by Kitaev-Heisenberg paramagnons, *Physical Review B* **99**, 085136 (2019).